ARMY RESEARCH LABORATORY

Characterization of Pressureless Sintered Boron Carbide

by Joshua Pomerantz and Tomoko Sano

ARL-TR-6391 **March 2013**

NOTICES

Disclaimers

The findings in this report are not to be construed as an official Department of the Army position unless so designated by other authorized documents.

Citation of manufacturer's or trade names does not constitute an official endorsement or approval of the use thereof.

Destroy this report when it is no longer needed. Do not return it to the originator.

Army Research Laboratory
Aberdeen Proving Ground, MD 21005-5069

ARL-TR-6391 **March 2013**

Characterization of Pressureless Sintered Boron Carbide

Joshua Pomerantz
George Washington University

Tomoko Sano
Weapons and Materials Research Directorate, ARL

REPORT DOCUMENTATION PAGE	Form Approved OMB No. 0704-0188

1. REPORT DATE *(DD-MM-YYYY)*	2. REPORT TYPE	3. DATES COVERED (From - To)
March 2013	Final	June 2012–August 2012

4. TITLE AND SUBTITLE
Characterization of Pressureless Sintered Boron Carbide

5a. CONTRACT NUMBER

5b. GRANT NUMBER

5c. PROGRAM ELEMENT NUMBER

6. AUTHOR(S)
Joshua Pomerantz* and Tomoko Sano

5d. PROJECT NUMBER

5e. TASK NUMBER

5f. WORK UNIT NUMBER

7. PERFORMING ORGANIZATION NAME(S) AND ADDRESS(ES)
U.S. Army Research Laboratory
ATTN: RDRL-WMM-B
Aberdeen Proving Ground, MD 21005-5069

8. PERFORMING ORGANIZATION REPORT NUMBER
ARL-TR-6391

9. SPONSORING/MONITORING AGENCY NAME(S) AND ADDRESS(ES)

10. SPONSOR/MONITOR'S ACRONYM(S)

11. SPONSOR/MONITOR'S REPORT NUMBER(S)

12. DISTRIBUTION/AVAILABILITY STATEMENT
Approved for public release; distribution is unlimited.

13. SUPPLEMENTARY NOTES
*George Washington University, 2100 M Street, #310, Washington, DC 20052

14. ABSTRACT
This report outlines the characterization study of pressureless sintered boron carbide with graphite additive used as a sintering and densification aid on hexagonally shaped and plate-shaped samples of boron carbide. We conducted this investigation to determine whether pressureless sintered boron carbide could be used as a substitute for the baseline hot-pressed boron carbide. The surfaces were characterized with a scanning electron microscope. The samples were tested for strength, hardness, density, and composition using four-point flexure testing, Knoop microindentation, Archimede's method, and x-ray spectroscopy, respectively. These values were then compared with literature values for pressureless sintered boron carbide and hot-pressed boron carbide. We concluded that the substitution was not feasible because of the high-porosity and low-strength values.

15. SUBJECT TERMS
boron carbide, ceramic, characterization, material

16. SECURITY CLASSIFICATION OF:			17. LIMITATION OF ABSTRACT	18. NUMBER OF PAGES	19a. NAME OF RESPONSIBLE PERSON
a. REPORT	b. ABSTRACT	c. THIS PAGE			Joshua Pomerantz
Unclassified	Unclassified	Unclassified	UU	18	19b. TELEPHONE NUMBER (*Include area code*) 410-306-2741

Standard Form 298 (Rev. 8/98)
Prescribed by ANSI Std. Z39.18

Contents

List of Figures

List of Tables

Acknowledgments

The authors thank Dennis Miller, Paul Moy, Jared Wright, Costas Fountzoulas, and Corydon Hilton for their help on this project.

1. Introduction

The ceramic boron carbide (B_4C) has a rhomboahedral crystal structure, with icosahedra of either $B_{11}C$ or B_{12} located at each corner, connected to each other through C-B-C- intericosahedral chains. While $B_{11}C$ is more common, the replacement of the $B_{11}C$ icosahedra with the B_{12} icosahedra causes uncertainty in the stoichiometry of B_4C. It is possible for B_4C to exist as B_4C or $B_{13}C_3$, i.e., to have a carbon content ranging from ~9 atomic percent (at%) to 20 at% (*1*). With a Knoop hardness (HK) of 2800 kg/mm^2 at a load of 0.1 kgf (0.98 N), B_4C is the third hardest material in the world, softer than only cubic boron nitride and diamond (*2, 3*). This and its low theoretical density of 2.52 g/cm^3 make it a suitable ceramic for armor (*4*).

The B_4C used for body armor is normally consolidated by hot-pressing (HP). HP B_4C has a density near to the theoretical density; however, HP is slow, and products can be molded into only simple shapes. HP B_4C is normally machined into its proper shape, a costly and inefficient process. Recently, B_4C has been pressurelessly sintered without pressure using several different additives to increase densification. These additives, however, have a detrimental effect on the mechanical properties of B_4C (*1*). Even with the additives, pressureless sintered B_4C can still have a high porosity—another factor inhibiting its mechanical performance. For example, the most common additive, free carbon (graphite), increases densification up to 98% of the theoretical density (*5*) (2.47 g/cm^3). However, its softness and inhomogeneous distributions lower the hardness of the B_4C in areas with a high concentration of graphite.

The purpose of this research is to determine the feasibility of substituting pressureless sintered B_4C with graphite additives for HP of the same material for use in armor. If the pressureless sintered B_4C demonstrates comparable performance, then the reduced cost of sintering, machining, and processing, as well as the time spent on each step, may justify such a substitution. This study characterizes pressureless sintered B_4C with graphite additives and compares the results to the literature values for HP B_4C.

2. Experimental/Calculations

This study evaluated pressureless sintered B_4C samples with graphite additions, which have been manufactured in Spain into two shapes: hexagonal and plate. Both shapes are characterized in this study to be compared with the literature values.

Specimen densities of both hexagonal and plate samples were determined using the Archimedes method. The dry mass, wet mass, and suspended wet mass were measured using a Mettler Toledo Deller Range AX250 scale. Specimens were placed into a vacuum chamber for 45 min

then submerged in water for 1 h before the wet and suspended wet mass measurements were taken. The apparent density was calculated according to the equation

$$\rho_a = \frac{DM}{DM - SWM}, \quad (1)$$

where ρ_a is the apparent density, *DM* is the dry mass, and *SWM* is the suspended wet mass.

The surfaces of the B_4C samples were characterized under a scanning electron microscope (SEM) (FEI Nova NanoSEM 600). Elemental maps of the locations of elements present were determined by energy-dispersive spectroscopy (EDS). Elemental spectra and qualitative values of elemental content were also obtained. X-ray diffraction (XRD; Siemens 05005) was used to determine the phases present.

Grain boundary size was measured using the Heyn method (lineal intercept procedure) as outlined in section 11 of the ASTM E 112 (*6*) standard. The ASTM grain size number *n* was calculated according to ASTM E 112, equation 2a.

The flexural strength of the plate sample was tested at a room temperature of 25 °C using four-point flexure testing on 52 samples machined (Bomas Machine Specialties, Inc., Somerville, MA) to dimensions of 3 × 4 × 48 mm. The specimens were loaded into a load frame (Instron 5500R Model) with a lower support span of L = 40 mm and an upper support span of U = 20 mm. Specimens were loaded at a rate of 0.5 mm/min, and the break force *P* was recorded to six significant figures, as reported by the software (Bluehill). To ensure the greatest accuracy, the width *B* and thickness *D* of each specimen were measured at three points along the length of the sample and averaged. The average width and thickness of each specimen were used in the calculation of the respective specimen's strength. The strength of each individual sample was calculated according to the equation

$$S = \frac{3PL}{4BD^2}, \quad (2)$$

where *S* is the strength of the material, *P* is the break force in N, *L* is the outer support span in millimeters, *B* is the specimen width in millimeters, and *D* is the specimen thickness in millimeters (*7*). The values for the strength of each sample were then averaged to approximate the strength of the material. All tests were completed according to ASTM C 1161 (*7*). The flexural strength of the hexagonal specimen was not measured because of sample size limitations.

Samples were cold-mounted (Buehler Epoease Epoxy Mounting System) in 0.25-in (0.64-cm) silicone molds and left to harden for 8 h. They were then polished (Struers RotoPo-31 with RotoForce 4 attachment) using water-based diamond suspensions (Metadi Diamond suspensions) of decreasing size: 45, 15, 9, 6, 3, 1, and 0.25 µm. Subsequent to polishing, the samples were subjected to Knoop microindentation (Instron Wilson Tukon 2100 Version 95.42). The loads of

the indents were applied for increments of 13 s and steadily increased in the order 0.1, 0.3, 0.5, 1.0, 2.5 kg. The software (Minuteman) reported HK in terms of kg/mm^2, so no calculations were necessary. Ten indents which meet the criteria for "acceptable" in the ASTM were taken. The HK of each indent was recorded and averaged to approximate the HK of the material at each load. The data was plotted in a load-HK curve.

3. Results

The dry mass, wet mass, and suspended wet mass of the plate and hexagonal samples were 10.902, 11.088, and 6.355 g and 17.325, 17.427, and 10.052 g, respectively. Using these values in equation 1, we calculated the density of the plate sample to be 2.40 g/cm^3 and the hexagonal sample to be 2.38 g/cm^3.

SEM revealed both high porosity and graphite content in both samples. In figure 1, the imperfections on the surface were analyzed by EDS to be almost pure carbon. Further EDS analysis showed this graphite to account for a significant amount of the carbon content. Table 1 summarizes the qualitative characterization of the surface of the B_4C samples.

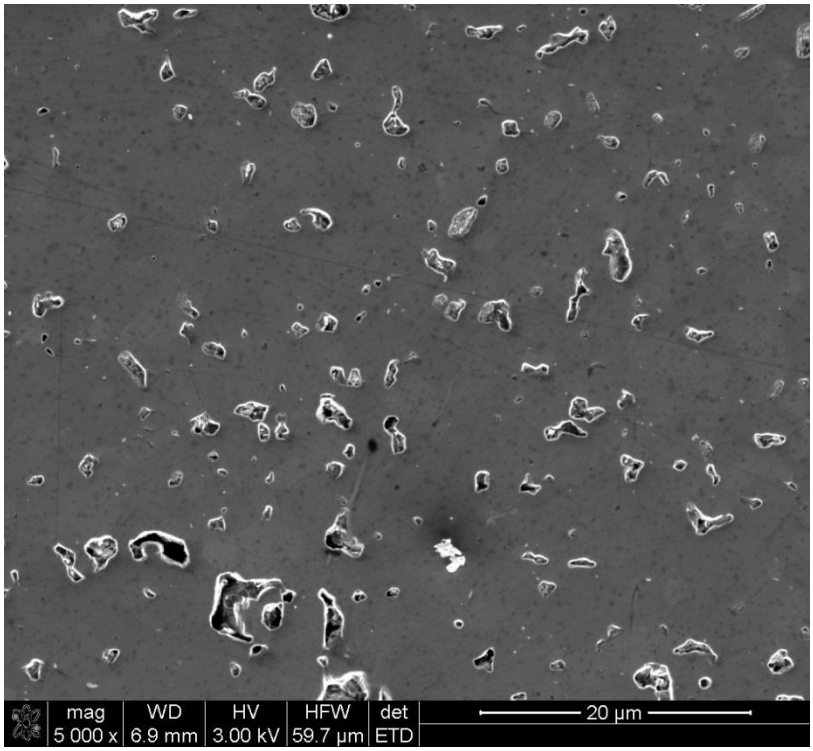

Figure 1. SEM image of a plate surface (polished 0.25 µm).

Table 1. EDS characterization of the samples.

Element	Plate Wt %	Plate At%	Hex. Wt%	Hex. At%
B	76.74	78.60	75.61	77.51
C	23.08	21.28	24.33	22.45
O	0.18	0.13	0.06	0.04

XRD spectra showed the phases present to be solely B_4C, proving the samples' purity. This data is represented by the XRD graph in figure 2.

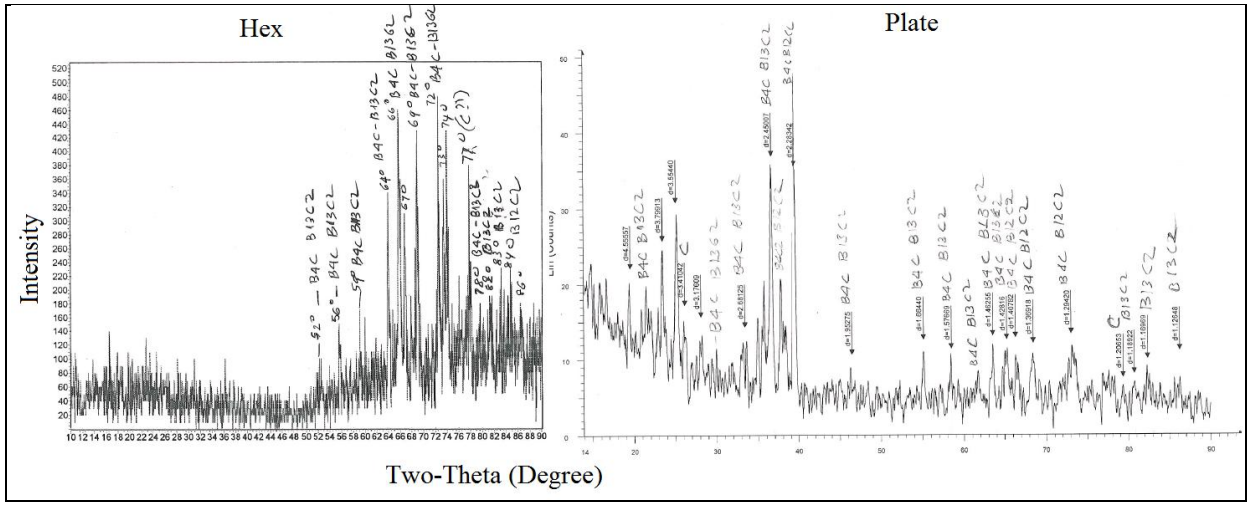

Figure 2. XRD results.

The ASTM grain size numbers of the plate sample and the hexagonal sample were calculated to be ~15 and 14, respectively

Four-point flexure testing yielded an average strength of 295 ± 38 MPa. The 52 individual strengths are represented in a scatter plot figure 3, with the error bars representing the standard deviation (38). The strongest specimen had a break force of –440.4 N, and the weakest specimen had a break force of –253.6 N. SEM micrographs revealed pores, one of which is shown in figure 4, at the initiation site of the fractures. The mode of fracture was transgranular, indicating a strong grain boundary.

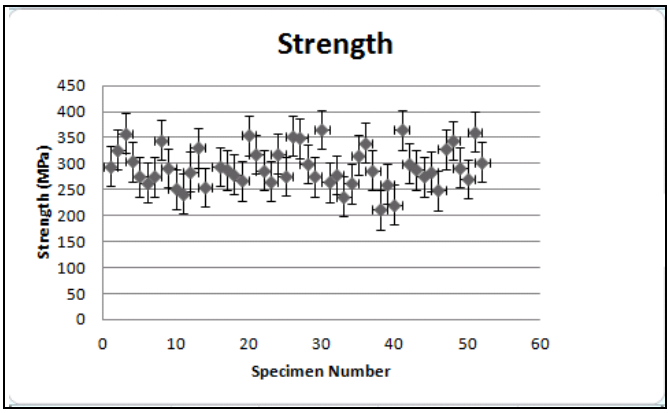

Figure 3. Strength scatter plot.

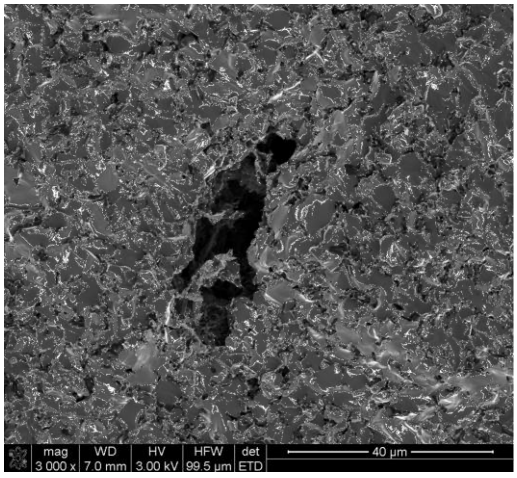

Figure 4. SEM of pore in the weakest sample.

Both samples had approximately the same HK values within experimental error. The load-HK plot is shown in figure 4. The HK of the plate sample at a 1-kgf (9.8 N) load was 2051 ± 182.2 kg/mm^2. The HK of the hexagonal at the same load was 2187 ± 78.25 kg/mm^2. As seen in figure 5, HK decreases as the load increases. The error bars in this figure represent the standard deviation. Above loads of 2.5 kgf, several indentations would strike a pore and cause laceration and cracking.

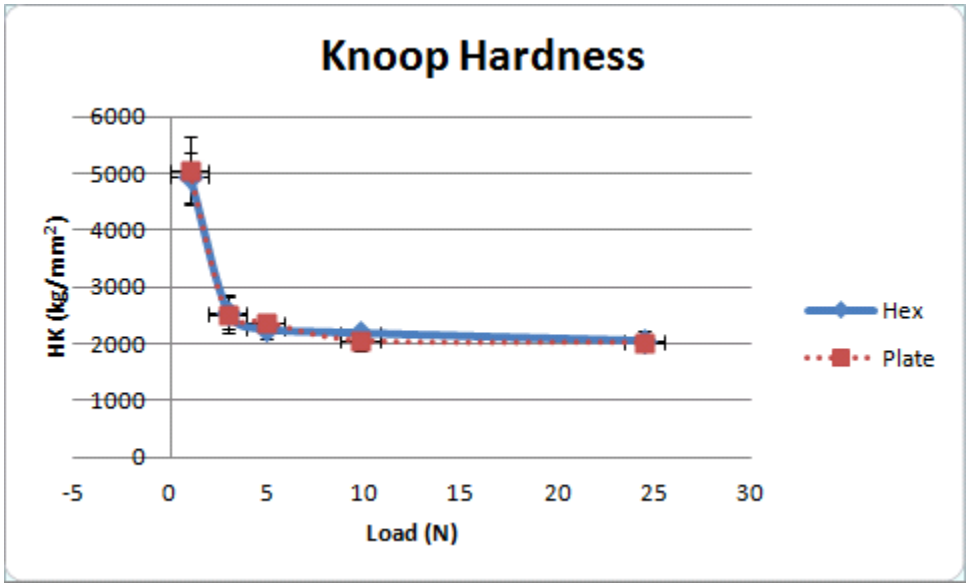

Figure 5. Load-HK curve.

4. Discussion

As mentioned in the introduction, the theoretical density of B_4C is 2.52 g/cm^3. The measured densities of the B_4C hexagonal and plate samples were 95.2% and 94.4% of the theoretical density, respectively. These values indicate a high densification; HP is normally required for densities above 95% of the theoretical density (*1*). Despite this high densification, however, porosity is still observed under the SEM, and because the porosity had a detrimental effect on the mechanical properties of the samples, it is questionable as to whether this material can be used as an armor material.

SEM imaging revealed large chunks of graphite distributed throughout the material. An effect of this graphite is seen in the high standard deviation in the HK test. Since the graphite is inhomogenously distributed, certain areas will have more graphite than others. As graphite is softer than B_4C, the HK measured in these areas is smaller. Areas with moderate amounts of graphite have a higher HK, and areas with little graphite have the highest HK values. This difference makes the HK of an area of the material unpredictable. EDS results are normal within experimental error; variations in carbon could be due to graphite or surface contamination, and the negligible amounts of oxygen detected are most likely due to oxidation.

The average flexural strength of HP B_4C is 480 ± 40 MPa (*8*). The significant difference between this value and the strength of the plate sample is most likely caused by the high porosity; pores were determined to be the nucleation site of the fracture of two flexure samples, the sample that fractured at the highest load and the one at the lowest load.

Despite the high standard deviation in the HK test, the average HK values of the samples were high. The values of the plate and hexagonal samples compared to the value of HP B_4C at 100% theoretical density, which is 2019.9 ± 60.2 kg/mm^2 at 1 kgf (9.8 N) (*8*).

5. Summary and Conclusions

Whether pressureless sintered B_4C can be a substitute for HP B_4C for armor applications remains undetermined. This study's specimens' low density and high hardness certainly show potential; however, their high porosity and graphite content have too detrimental an effect on the mechanical properties (such as strength) for the lowered cost and time of manufacturing to be justified. If the densification can be increased, then substitution is plausible. Ballistic testing of the pressureless sintered samples is necessary to conclusively determine the feasibility of the substitution. Table 2 summarizes the mechanical properties evaluated in this study.

Table 2. Summary of the mechanical properties evaluated in this study.

Sample	**ρ (g/cm^3)**	**Strength (MPa)**	**HK (9.8 N; kg/mm^2)**
Hex	2.38	—	2187 ± 78.25
Plate	2.40	295 ± 38	2051 ± 182.2
HP Lit.	2.52	480 ± 40	2019.9 ± 60.2

6. References

1. Thévenot, F. Boron Carbide—A Comprehensive Review. *Journal of the European Ceramic Society* **1990**, *6*, 205–225.
2. Cho, N. Processing of Boron Carbide. Ph.D. dissertation, Georgia Institute of Technology, Atlanta, GA, 2006.
3. Bever, M. B., Ed. *Encyclopedia of Materials Science and Engineering*; MIT Press: Cambridge, MA, 1986; Vol. 1.
4. Roy, T. K.; Subramanian, C.; Suri, A. K. Pressureless Sintering of Boron Carbide. *Ceramics International* **2006**, *32*, 227–233.
5. Schwetz, K.; Vogt, G. Process for the Production of Dense Sintered Articles of Boron Carbide. U.S. Patent 4,195,066, March 25, 1980.
6. ASTM E 112. Standard Test Methods for Determining Average Grain Size. *Annu. Book ASTM Stand*. **2007**.
7. ASTM C 1161. Standard Test Method for Flexural Strength of Advanced Ceramics at Ambient Temperature. *Annu. Book ASTM Stand*. **2007**.
8. Gonzalez, L. V.; Speyer, R. F.; Campbell, J. Flexural Strength, Fracture Toughness, and Hardness of Silicon Carbide and Boron Carbide Armor Ceramics. *International Journal of Applied Ceramic Technology* **2010**, *7* (5) 643–651.

NO. OF
COPIES ORGANIZATION

1 (PDF) DEFENSE TECHNICAL INFORMATION CTR
DTIC OCA
8725 JOHN J KINGMAN RD
STE 0944
FORT BELVOIR VA 22060-6218

1 (HC) DIRECTOR
US ARMY RESEARCH LAB
IMAL HRA
2800 POWDER MILL RD
ADELPHI MD 20783-1197

1 (PDF) DIRECTOR
US ARMY RESEARCH LAB
RDRL CIO LL
2800 POWDER MILL RD
ADELPHI MD 20783-1197

1 (PDF) GOVT PRINTG OFC
A MALHOTRA
732 N CAPITOL ST NW
WASHINGTON DC 20401

ABERDEEN PROVING GROUND

3 (PDF) DIR USARL
RDRL WMM B
C RANDOW
RDRL WMM E
J LASALVIA
J SWAB

INTENTIONALLY LEFT BLANK.